



Published in final edited form as:

Nature. 2010 December 16; 468(7326): 964–967. doi:10.1038/nature09570.

Noise correlations improve response fidelity and stimulus encoding

Jon Cafaro² and Fred Rieke^{1,2,*}

¹ Howard Hughes Medical Institute, University of Washington, Seattle, WA 98195

² Department of Physiology and Biophysics, University of Washington, Seattle, WA 98195

Abstract

Computation in the nervous system often relies on the integration of signals from parallel circuits with different functional properties. Correlated noise in these inputs can, in principle, have diverse and dramatic effects on the reliability of the resulting computations^{1–8}. Such theoretical predictions have rarely been tested experimentally because of a scarcity of preparations that permit measurement of both covariation of a neuron's input signals and the effect of manipulating such covariation on a cell's output. Here we introduce a new method to measure covariation of the excitatory and inhibitory inputs a cell receives. This method revealed strong correlated noise in the inputs to two types of retinal ganglion cell. Eliminating correlated noise without changing other input properties substantially decreased the accuracy with which a cell's spike outputs encoded light inputs. Thus covariation of excitatory and inhibitory inputs can be a critical determinant of the reliability of neural coding and computation.

Differences in the properties of excitatory and inhibitory synaptic inputs to a target cell provide a key control of neural activity. Feedforward inhibitory synaptic input is a ubiquitous example. A delay in inhibitory input relative to excitatory input, e.g. by an extra synaptic delay in the circuit providing inhibitory input, can limit response duration to the time window in which the target cell receives excitatory but not inhibitory input⁹. More generally, inhibitory input can cancel unwanted responses by arriving prior to or at the same time as excitatory input^{10–13}. Theoretical work illustrates how the effectiveness of these computations depends on the strength of covariation between excitatory and inhibitory synaptic inputs⁸. Thus while synaptic noise will always decrease the reliability of the neural response, strong noise correlations, unlike independent noise, could allow fluctuations in inhibitory synaptic input to cancel corresponding fluctuations in excitatory synaptic input⁵ (Fig. 1). Such noise correlations can arise if noise within excitatory and inhibitory pathways originates from a common source (Fig. 1, left) - e.g. in densely and randomly connected

Users may view, print, copy, download and text and data- mine the content in such documents, for the purposes of academic research, subject always to the full Conditions of use: http://www.nature.com/authors/editorial_policies/license.html#terms

Correspondence and requests for material should be addressed to F.R. (rieke@u.washington.edu).

Author Contributions: J.C. and F.R. participated in all aspects of this work.

Author Information: Reprints and permissions information is available at www.nature.com/reprints. The authors declare no competing financial interests.

recurrent networks¹⁴. Noise cancellation in synaptic integration could in turn reduce trial-to-trial variability in a cell's spike output (Fig. 1, right).

The extent and impact of noise correlations depends on several network and cellular properties, including nonlinearities in synaptic transmission¹⁵ or spike generation¹⁶ which could decrease correlation strength. This dependence makes it difficult to predict the importance of noise correlations from modeling alone or from correlations measured in cell pairs. Work in the retina provides a rare opportunity to provide quantitative experimental information about how noise correlations effect the coding of physiologically relevant stimuli. Our goal was to first measure covariation of the excitatory and inhibitory synaptic inputs received by a retinal ganglion cell (Fig. 1, ①) and then test how these noise correlations impact the encoding of light stimuli in a cell's spike output (Fig. 1, ②).

Quantifying covariation of excitatory and inhibitory synaptic input requires measuring these two conductances simultaneously or near simultaneously. To do this, we rapidly alternated the ganglion cell voltage between the reversal potentials for excitatory and inhibitory synaptic input, collecting a single sample of each input every 10 ms (Fig. 2a). Control experiments indicated that the voltage at the synaptic receptors had reached a near-constant value at these sampling times (Supplementary Fig. 1). This sampling rate is fast compared to the 50–100 ms time course of a ganglion cell's response to light inputs. To check how well this procedure captured light-dependent changes in conductance, we compared the simultaneously measured conductances with those measured non-simultaneously when the voltage was held constant at the excitatory or inhibitory reversal potential. Mean excitatory and inhibitory conductances to a repeated, modulated light input differed minimally (Fig. 2b). In 21 cells, the alternating voltage approach captured $99.9 \pm 0.6\%$ of the power of the conductance signal and $83 \pm 4\%$ of that of the conductance noise (mean \pm SEM, see Methods). Thus simultaneous conductance measurements capture most of the structure in the synaptic inputs a ganglion cell receives.

Simultaneous conductances measured during constant light often exhibited spontaneous excitatory synaptic events accompanied in time by inhibitory synaptic events (Fig. 2c₁, black arrow heads). Such events in fact typically occurred together. Correlated noise events were rarely observed during non-simultaneously measured conductances (Fig. 2c₂). Correspondingly, the cross-correlation function for simultaneously measured excitatory and inhibitory conductances during constant light showed considerable structure, unlike the cross correlation for non-simultaneously measured conductances (single cell Fig. 2d₁, population Fig. 2d₂). Thus simultaneous conductance recordings revealed correlations between converging synaptic inputs that were inaccessible from more conventional recordings.

How strong are noise correlations during modulated light and what impact do they have on a cell's spike output? We answered these questions first for midget ganglion cells, which comprise the majority of ganglion cells in the primate retina¹⁷. Midget ganglion cells receive delayed feedforward synaptic inhibition, where the delay reflects an extra synapse in the circuit controlling inhibitory input. Thus excitatory input originates directly from bipolar cells, while inhibitory input originates from amacrine cells that themselves receive input

from bipolar cells¹⁸. Similar delayed feedforward inhibition is a characteristic of many cortical circuits, including hippocampus, cerebellum, barrel cortex, and auditory cortex^{9,11,12,19-21}. We simultaneously recorded excitatory and inhibitory synaptic input during a full field modulated light stimulus (Fig. 3a₁) and estimated variability in the synaptic responses by subtracting the average synaptic input from each individual trial (Fig. 3a₂). The peak correlation strength of the resulting residuals ranged from 0.15 to 0.5 (Fig. 3b₁ and b₂, black traces). Noise correlations in the interleaved non-simultaneous conductances were substantially smaller (Fig. 3b₁ and b₂, green traces). Slow drift in the light response accounted for the remaining noise correlations in the non-simultaneous conductances (Supplementary Fig. 2).

The alternating voltage technique could produce artifactual noise correlations by overshooting the appropriate reversal potentials for excitatory or inhibitory synaptic input. For example, holding at a voltage positive to the excitatory reversal potential could cause an increase in the excitatory conductance to be misinterpreted as an increase in both the excitatory and inhibitory conductance, thus leading to an artifactual correlation. A similar logic holds if a cell is held more negative than the reversal potential for inhibitory input. However, if anything the alternating voltage technique fell short of the actual reversal potentials and hence underestimated the strength of noise correlations (Supplementary Fig. 3).

What impact does covariation of excitatory and inhibitory synaptic inputs have on a midretinal ganglion cell's response to physiological inputs? We answered this question by comparing the pattern of spikes produced by simultaneous (with noise correlations) and non-simultaneous (without noise correlations) conductances in dynamic clamp experiments (Fig. 3c, Supplementary Fig. 4). The non-simultaneous conductances consisted of shuffled pairings of simultaneously recorded excitatory and inhibitory conductances; this procedure removed noise correlations while holding all other statistics constant. We compared the precision of the spike responses to the two sets of conductances by calculating the signal-to-noise ratio from repeated dynamic clamp trials (Fig. 3d, see Methods). In all cases the signal-to-noise ratio was higher for conductances with noise correlations (Fig. 3e). Quantifying the temporal precision of the spike responses using a spike distance metric^{22,23} gave similar results (data not shown). Thus the precision of a midretinal ganglion cell's output in response to light stimuli depends on covariation of excitatory and inhibitory synaptic inputs.

Feedforward synaptic inhibition can serve a more diverse functional role when the amplitude or timing of inhibitory input relative to excitatory input depends on the stimulus. For example, the ability of a subset of retinal ganglion cells to respond to the direction of a moving object^{24,25} (Fig. 4a and b) relies on cancellation of excitatory input by inhibitory input in the non-preferred direction¹⁰. Covariation of excitatory and inhibitory synaptic inputs could make such a mechanism robust to noise - e.g. by preventing a larger than average excitatory synaptic event from overwhelming the corresponding inhibitory synaptic event and causing a response to movement in an inappropriate direction. To test this proposal, we recorded simultaneous conductances in mouse On-Off directionally-selective ganglion cells (On-Off DSGCs) in response to a bar of light moving in different directions (Fig. 4a). Excitatory and inhibitory conductances showed strong noise correlations that were

largely absent in non-simultaneous conductances (Fig. 4d; see Supplementary Fig. 5 for results from full-field light stimuli). Both excitatory and inhibitory conductances and the strength of the noise correlations depended on bar direction (Fig 4c and d). For example, noise correlations in the non-preferred direction were 3–4 times stronger than those in the preferred direction. Further, excitatory and inhibitory conductances showed near perfect covariation in the non-preferred direction.

We tested the impact of noise correlations on direction tuning using simultaneous (with noise correlations) and non-simultaneous (without noise correlations) conductances in dynamic clamp experiments; non-simultaneous conductances consisted of simultaneous conductances shuffled between trials but not bar directions. Both the mean and standard deviation of the firing rate in the non-preferred direction were considerably higher for non-simultaneous conductances (Fig. 4e and f). The failure of a cell to reliably attenuate its response for movement in the non-preferred direction should negatively impact its ability to encode direction. Indeed, each recorded cell showed greater direction selectivity for the simultaneous conductances (Fig. 4g). Thus the computation underlying directional selectivity depends on covariation of excitatory and inhibitory synaptic inputs and the resulting cancellation of noise shared between the circuits providing each type of input.

Computation in the retina follows a basic plan found in many other neural circuits: signals in a common population of inputs diverge to parallel and functionally dissimilar pathways, and integration of the signals from multiple parallel pathways governs the output of the circuit. Divergence into separate excitatory and inhibitory circuits is a prominent example of such a motif. Noise in shared inputs naturally causes covariation of signals in the parallel pathways. The strength of such noise correlations will depend on cellular properties within the network^{15,16}, the stimulus delivered (see Fig 4)²⁶, and the state of the network²⁷. Thus excitatory and inhibitory inputs to cells in some, but not all, circuits are expected to show strong noise correlations, as indeed is the case in barrel cortex^{27,28}. Here, we put such noise correlations in the context of the coding of physiological relevant stimuli. Our results reveal a critical role for noise correlations in maintaining appropriate cancellation of excitatory and inhibitory inputs and thus sharpening tuning to specific stimuli. This work provides an important example of neurons that perform computations reliant on noise correlations. Given the prevalence of circuits in which feedforward inhibition shapes neural responses^{9,11,12,19–21}, noise correlations likely play a similar role in other neural circuits.

Methods Summary

Electrical recordings were made from midretinal ganglion cells in primate and On-Off DSGCs in mouse retinas using patch-clamp techniques as previously described^{23,29}. Light stimuli were delivered from LEDs or an OLED monitor (eMagin). Mean light levels for all experiments were near 5000 R*/cone/sec.

The 10 ms cycle period during the simultaneous conductance recordings allows us to resolve input at 50Hz and below. The fraction of the measured current variance at this cycle time was determined by calculating the fraction of the variance of the non-simultaneous (constant

voltage) conductances that can be accounted for by the variance of the simultaneous conductances.

Signal-to-noise ratios of spike outputs were calculated by forming spike trains of zeroes and ones from each trial with 1 ms resolution. The mean and trial residuals of these spike trains were calculated and the power spectrum of these functions were assessed and corrected for sample number bias³⁰. Power spectra were integrated between 1 and 20Hz and the sum of the mean power spectrum was divided by the sum of the residual power spectrum (Supplementary Fig. 6).

Spike number in On-Off DSGCs in response to moving bar was summed over the entire duration of the bars movement. The direction selective index¹⁰ was calculated as follows:

$$DSI = \left| \frac{\sum \vec{v}_i}{\sum r_i} \right|$$

where \vec{v}_i are vectors with length r_i , equal to the normalized firing rate, and pointing in the same direction of the moving bar that produced the presented conductances.

Current injected into a cell (I) during dynamic clamp experiments³¹ was calculated as indicated below.

$$I(t) = G_{exc}(t) * (V(t - \Delta t) - E_{exc}) + G_{inh}(t) * (V(t - \Delta t) - E_{inh})$$

Where G_{exc} and G_{inh} are a set of conductances recorded during light stimulation, V is the cells membrane potential, and E_{exc} and E_{inh} are reversal potentials set at 0 mV and -80 mV. Changing the inhibitory reversal potential to -50 mV did not substantially impact the results.

Methods

Electrical recordings were made from midget ganglion cells in primate and On-Off DSGCs in mouse retinas as previously described^{23,29}. Midget ganglion cells were identified by their relatively sustained response to light steps and characteristic morphology^{17,29,32}. On-Off DSGCs were identified by a combination of at least two of the following criteria: 1) an on-off light response to a brief light step, 2) bistratified morphology, or 3) direction selective spike response.

Light stimuli were delivered from LEDs or an LED monitor (eMagin). Mean light levels for all experiments were near 5000 R*/cone/sec. Full field stimuli consisted of 10 seconds of constant light followed by 10 seconds of 50% contrast modulated light (low pass filtered at 60 Hz) repeated for 5–20 trials. Moving bars were 180 μ m wide, 720 μ m long, moved at 864 μ m/sec along the long axis and had a contrast between 100–150%.

For all recordings a flat-mounted piece of retina was superfused with warmed (31–34° C) and oxygenated (5% CO₂/95% O₂) Ames solution. Midget cell dynamic clamp experiments were performed with receptors mediating excitatory and inhibitory synaptic input blocked (NBQX 10 μM, strychnine 1 μM, gabazine 10 μM). Pipettes for voltage-clamp recordings were filled with a Cs-based internal solution (105 mM CsCH₃SO₃, 10 mM TEA-Cl, 20 mM HEPES, 10 mM EGTA, 5 mM Mg-ATP, 0.5 mM Tris-GTP, and 2 mM QX-314; pH ~7.3, ~280 mOsm). Pipettes for dynamic clamp experiments were filled with a K-based internal solution (110 mM K Aspartate, 1 mM MgCl, 10 mM HEPES, 5 mM NMDG, 0.5 mM CaCl₂, 10 mM phosphocreatine, 4 mM Mg-ATP, and 0.5 Tris-GTP; pH ~7.2, ~280 mOsm). Liquid junction potentials were ~10 mV and were not compensated throughout the text. Low access resistance was critical, and only cells with access resistance below 20 MΩ; were included for analysis. Access resistance was partially compensated (75% for experiments using an Axopatch 200B amplifier; 50% compensation and prediction for experiments using a Multiclamp 700B amplifier). Conductances were derived from excitatory (inhibitory) synaptic currents by dividing the excitatory (inhibitory) current by an assumed driving force of –62 mV (+62 mV).

Both ganglion cell types showed evidence for NMDA-receptor mediated conductances (j-shaped I-V plots which became linear in the presence of 10 μM APV). The presence of an NMDA conductance could cause large underestimations of noise correlations in the event that we are substantially below the excitatory reversal potential. However, we observed only a weak impact of this conductance when noise correlations were compared before and after application of APV. Results from two cells recorded only in the presence of APV were included in the full data set.

The 10 ms cycle period during the simultaneous conductance recordings allows us to resolve input at 50Hz and below. The fraction of the measured current variance at this cycle time was determined by calculating the fraction of the variance of the non-simultaneous (constant voltage) conductances that can be accounted for by the variance of the simultaneous conductances.

Signal-to-noise ratio of spike outputs were calculated by forming spike trains of zeroes and ones from each trial with 1 ms resolution. The mean and trial residuals of these spike trains were calculated and the power spectrum of these functions were assessed and corrected for sample number bias³⁰. Power spectra were integrated between 1 and 20Hz and the sum of the mean power spectrum was divided by the sum of the residual power spectrum (Supplementary Fig. 6).

Spike number in On-Off DSGCs in response to moving bar was summed over the entire duration of the bars movement. The direction selective index¹⁰ was calculated as follows:

$$DSI = \left| \frac{\sum \vec{v}_i}{\sum r_i} \right|$$

where \vec{v}_i are vectors with length r_i , equal to the normalized firing rate, and pointing in the same direction of the moving bar that produced the presented conductances.

Current injected into a cell (I) during dynamic clamp experiments³¹ was calculated as indicated below.

$$I(t) = G_{exc}(t) * (V(t - \Delta t) - E_{exc}) + G_{inh}(t) * (V(t - \Delta t) - E_{inh})$$

Where G_{exc} and G_{inh} are a set of conductances recorded during light stimulation, V is the cells membrane potential, and E_{exc} and E_{inh} are reversal potentials set at 0 mV and -50 mV to -80 mV respectively. The exact inhibitory reversal potential did not substantially impact the highlighted results.

Correlations were calculated using the 'xcov' function supplied by Matlab (MathWorks, Natick, MA) and normalized using the 'coef' option. Briefly, this function calculates the cross correlation after subtracting the means off each trial and normalizes by the geometric mean of the autocorrelation (see supplemental eq. 2.1).

Supplementary Material

Refer to Web version on PubMed Central for supplementary material.

Acknowledgments

We thank D. Dacey, O. Packer, J. Crook, B. Peterson, and T. Haun for providing primate tissue; P. Newman and E. Martinson for technical assistance; T. Azevedo, E.J. Chichilnisky, F. Dunn, G. Murphy, S. Kuo, E. Shea-Brown, M. Shadlen, and W. Spain for comments on the manuscript and helpful discussions. Support was provided by HHMI and NIH (EY-11850).

References

1. Shadlen MN, Newsome WT. Noise, neural codes and cortical organization. *Curr Opin Neurobiol.* 1994; 4:569–579. [PubMed: 7812147]
2. Softky WR, Koch C. The highly irregular firing of cortical cells is inconsistent with temporal integration of random EPSPs. *J Neurosci.* 1993; 13:334–350. [PubMed: 8423479]
3. Abbott LF, Dayan P. The effect of correlated variability on the accuracy of a population code. *Neural Comput.* 1999; 11:91–101. [PubMed: 9950724]
4. Romo R, Hernandez A, Zainos A, Salinas E. Correlated neuronal discharges that increase coding efficiency during perceptual discrimination. *Neuron.* 2003; 38:649–657. [PubMed: 12765615]
5. Salinas E, Sejnowski TJ. Impact of correlated synaptic input on output firing rate and variability in simple neuronal models. *J Neurosci.* 2000; 20:6193–6209. [PubMed: 10934269]
6. Dan Y, Alonso JM, Usrey WM, Reid RC. Coding of visual information by precisely correlated spikes in the lateral geniculate nucleus. *Nat Neurosci.* 1998; 1:501–507. [PubMed: 10196548]
7. Nirenberg S, Carcieri SM, Jacobs AL, Latham PE. Retinal ganglion cells act largely as independent encoders. *Nature.* 2001; 411:698–701. [PubMed: 11395773]
8. Averbek BB, Latham PE, Pouget A. Neural correlations, population coding and computation. *Nat Rev Neurosci.* 2006; 7:358–366. [PubMed: 16760916]
9. Pouille F, Scanziani M. Enforcement of temporal fidelity in pyramidal cells by somatic feed-forward inhibition. *Science.* 2001; 293:1159–1163. [PubMed: 11498596]

10. Taylor WR, Vaney DI. Diverse synaptic mechanisms generate direction selectivity in the rabbit retina. *J Neurosci.* 2002; 22:7712–7720. [PubMed: 12196594]
11. Wilent WB, Contreras D. Dynamics of excitation and inhibition underlying stimulus selectivity in rat somatosensory cortex. *Nat Neurosci.* 2005; 8:1364–1370. [PubMed: 16158064]
12. Wehr M, Zador AM. Balanced inhibition underlies tuning and sharpens spike timing in auditory cortex. *Nature.* 2003; 426:442–446. [PubMed: 14647382]
13. Leary CJ, Edwards CJ, Rose GJ. Midbrain auditory neurons integrate excitation and inhibition to generate duration selectivity: an in vivo whole-cell patch study in anurans. *J Neurosci.* 2008; 28:5481–5493. [PubMed: 18495882]
14. Renart A, et al. The asynchronous state in cortical circuits. *Science.* 2010; 327:587–590. [PubMed: 20110507]
15. Trong PK, Rieke F. Origin of correlated activity between parasol retinal ganglion cells. *Nat Neurosci.* 2008; 11:1343–1351. [PubMed: 18820692]
16. de la Rocha J, Doiron B, Shea-Brown E, Josic K, Reyes A. Correlation between neural spike trains increases with firing rate. *Nature.* 2007; 448:802–806. [PubMed: 17700699]
17. Dacey DM, Petersen MR. Dendritic field size and morphology of midget and parasol ganglion cells of the human retina. *Proc Natl Acad Sci U S A.* 1992; 89:9666–9670. [PubMed: 1409680]
18. Calkins DJ, Sterling P. Absence of spectrally specific lateral inputs to midget ganglion cells in primate retina. *Nature.* 1996; 381:613–615. [PubMed: 8637598]
19. Gabernet L, Jadhav SP, Feldman DE, Carandini M, Scanziani M. Somatosensory integration controlled by dynamic thalamocortical feed-forward inhibition. *Neuron.* 2005; 48:315–327. [PubMed: 16242411]
20. Luna VM, Schoppa NE. GABAergic circuits control input-spike coupling in the piriform cortex. *J Neurosci.* 2008; 28:8851–8859. [PubMed: 18753387]
21. Mittmann W, Koch U, Hausser M. Feed-forward inhibition shapes the spike output of cerebellar Purkinje cells. *J Physiol.* 2005; 563:369–378. [PubMed: 15613376]
22. Victor JD, Purpura KP. Nature and precision of temporal coding in visual cortex: a metric-space analysis. *J Neurophysiol.* 1996; 76:1310–1326. [PubMed: 8871238]
23. Murphy GJ, Rieke F. Network variability limits stimulus-evoked spike timing precision in retinal ganglion cells. *Neuron.* 2006; 52:511–524. [PubMed: 17088216]
24. Barlow HB, Hill RM, Levick WR. Retinal ganglion cells responding selectively to direction and speed of image motion in the rabbit. *J Physiol.* 1964; 173:377–407. [PubMed: 14220259]
25. Weng S, Sun W, He S. Identification of ON-OFF direction-selective ganglion cells in the mouse retina. *J Physiol.* 2005; 562:915–923. [PubMed: 15564281]
26. Cohen MR, Newsome WT. Context-dependent changes in functional circuitry in visual area MT. *Neuron.* 2008; 60:162–173. [PubMed: 18940596]
27. Gentet LJ, Avermann M, Matyas F, Staiger JF, Petersen CC. Membrane potential dynamics of GABAergic neurons in the barrel cortex of behaving mice. *Neuron.* 2010; 65:422–435. [PubMed: 20159454]
28. Okun M, Lampl I. Instantaneous correlation of excitation and inhibition during ongoing and sensory-evoked activities. *Nat Neurosci.* 2008; 11:535–537. [PubMed: 18376400]
29. Dunn FA, Lankheet MJ, Rieke F. Light adaptation in cone vision involves switching between receptor and post-receptor sites. *Nature.* 2007; 449:603–606. [PubMed: 17851533]
30. van Hateren JH, Snippe HP. Information theoretical evaluation of parametric models of gain control in blowfly photoreceptor cells. *Vision Res.* 2001; 41:1851–1865. [PubMed: 11369048]
31. Sharp AA, O’Neil MB, Abbott LF, Marder E. Dynamic clamp: computer-generated conductances in real neurons. *J Neurophysiol.* 1993; 69:992–995. [PubMed: 8463821]
32. Polyak S, Willmer EN. Retinal structure and colour vision. *Doc Ophthalmol.* 1949; 3:24–56. [PubMed: 18148793]

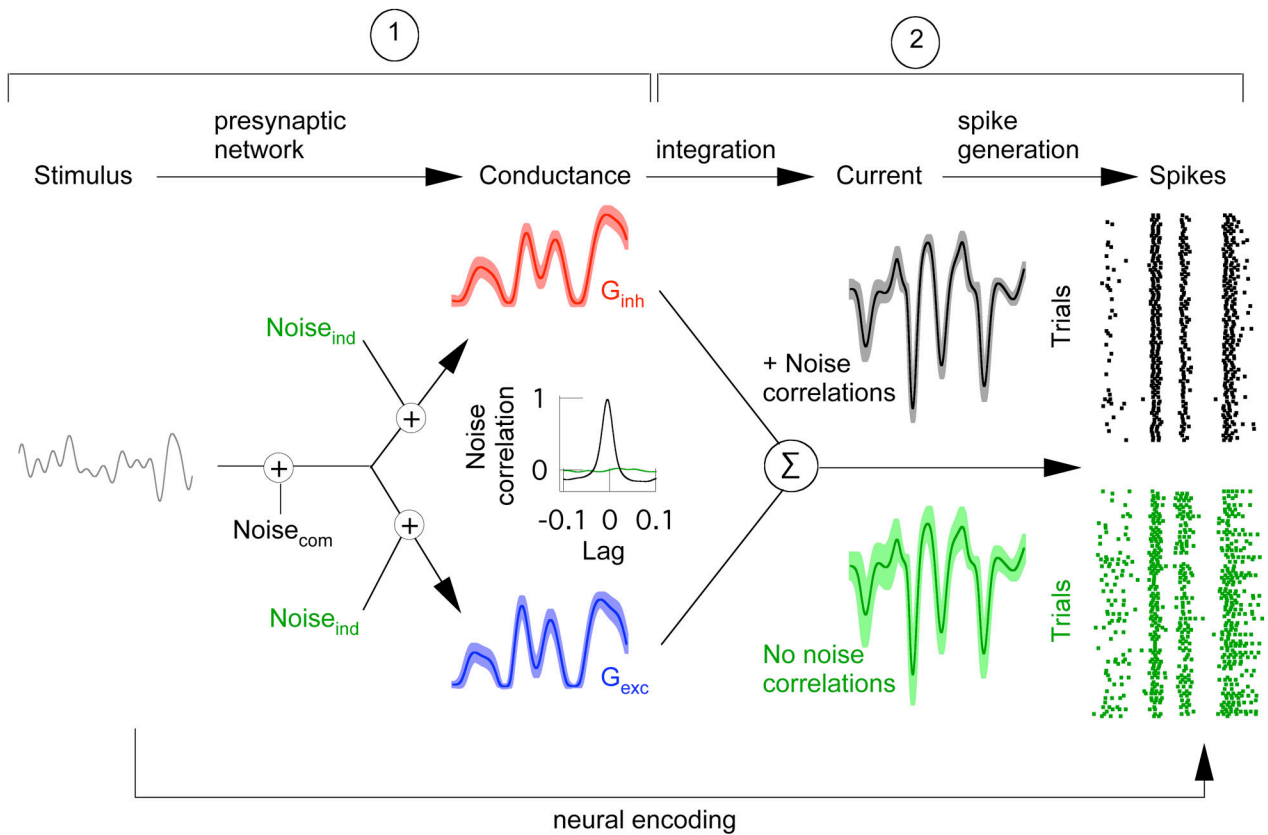


Figure 1.

Model illustrating effects of noise correlations on the variability of synaptic current and spike output. Neural encoding consists of three basic steps: a stimulus shapes excitatory (blue: G_{exc}) and inhibitory (red: G_{inh}) synaptic conductances; these conductances then shape synaptic currents; and the resulting currents control spike generation to produce a sequence of action potentials (spikes). Noise correlations will be strong if a common source dominates noise in excitatory and inhibitory pathways ($Noise_{com}$) and minimal if the dominant noise source arises independently ($Noise_{ind}$). Correlated (black traces) as opposed to uncorrelated (green traces) noise between excitatory and inhibitory conductances can lead to lower variability of both the synaptic current and spike output (shaded regions around traces). Understanding this issue requires answering two questions: ① How much do converging excitatory and inhibitory input covary? ② What is the impact of such noise correlations on the neural output?

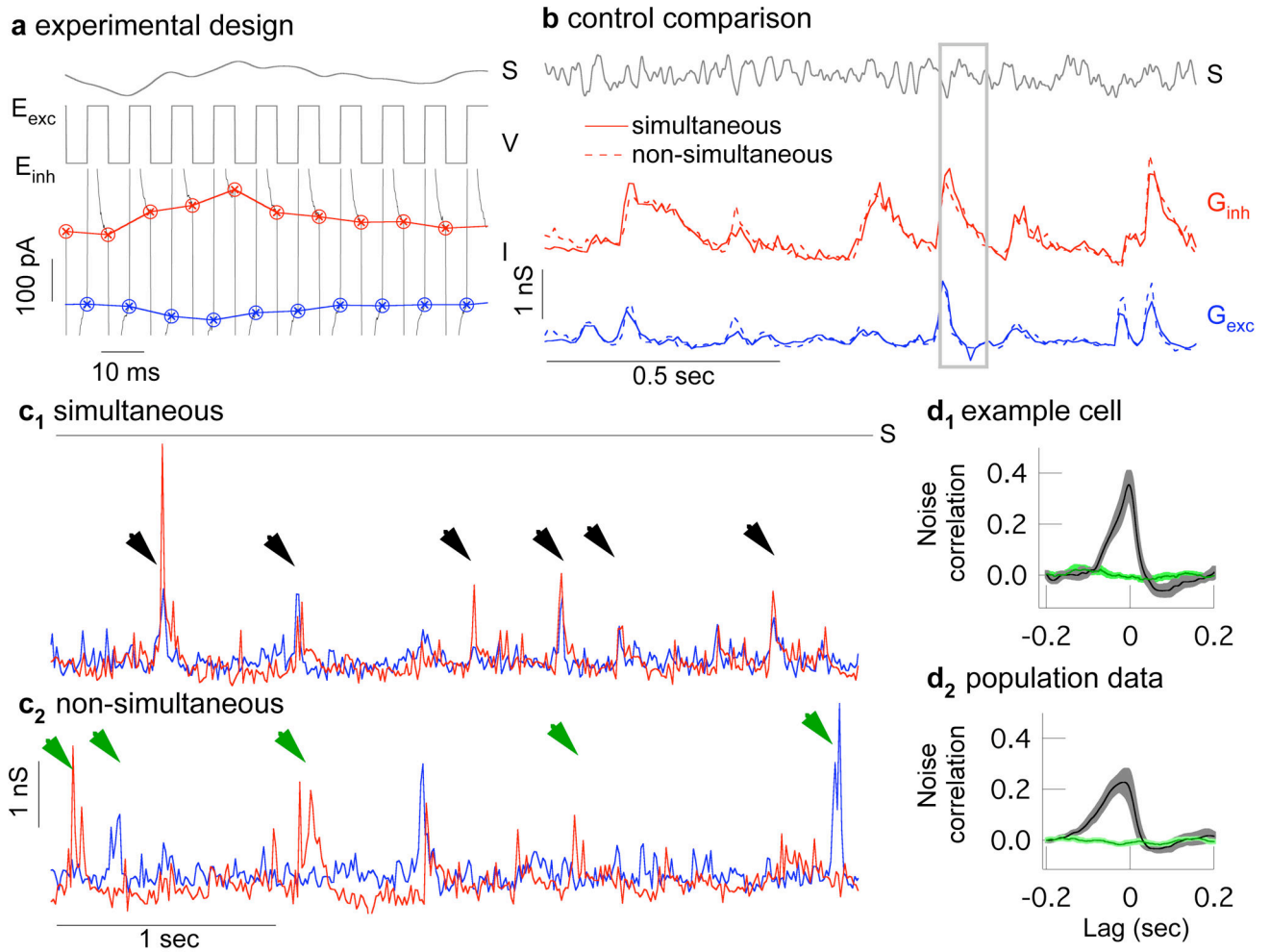


Figure 2.

Near-simultaneous recording of excitatory and inhibitory synaptic input to an On-Off directionally-selective ganglion cell. **a**, A light stimulus (S) is presented while the voltage (V) of the cell alternates between the excitatory and inhibitory reversal potentials (E_{exc} , E_{inh}). Excitatory (blue) and inhibitory (red) synaptic currents (I) are sampled at the end of each voltage step. **b**, Conductances derived from measured currents (see Methods) and averaged across multiple repeats of the same stimulus (S). Simultaneously-measured conductances (solid lines) closely match those measured non-simultaneously with the voltage held fixed at the reversal potentials for excitatory or inhibitory input (dashed lines, both excitatory and inhibitory correlations are 0.91 ± 0.01 , mean \pm sem, 21 cells). Panel **a** is a subsection of **b** (gray box). **c₁**, Section of simultaneously recorded conductances during constant light shows correlated excitatory and inhibitory spontaneous events (black arrow heads). **c₂**, Non-simultaneously recorded conductances also show spontaneous events (green arrow heads) but they are rarely correlated. Records have been resampled at 50 Hz for comparison with **c₁**. **d₁**, Cross correlation (mean \pm s.e.m, 10 trials) of excitatory and inhibitory conductances in an example cell during simultaneous (black) and non-

simultaneous recording (green). d_2 , Cross correlation for all recorded cells (mean \pm s.e.m, 6 cells).

Author Manuscript

Author Manuscript

Author Manuscript

Author Manuscript

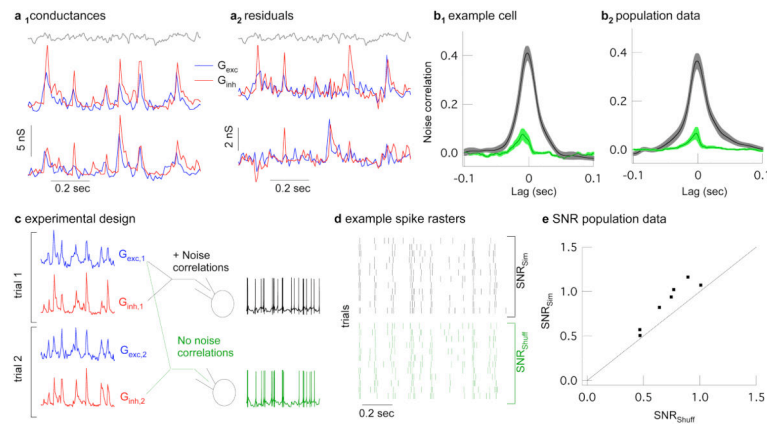


Figure 3. Strength and impact of noise correlations in synaptic inputs to primate midget ganglion cells. **a₁**, Two trials of simultaneously recorded conductances during modulated light (gray). **a₂**, Residual conductances (trials from **a₁** with mean subtracted), which estimate noise on each trial. **b₁**, Cross correlation (mean \pm sem, 12 trials) of excitatory and inhibitory residual conductances in an example cell during simultaneous (black) and non-simultaneous recording (green). **b₂**, Cross correlation for all recorded cells (mean \pm sem., 15 cells). **c**, Logic of dynamic clamp experiments using simultaneously or shuffled simultaneous conductances in place of synaptic input. **d**, Example spike trains from 12 dynamic-clamp trials of simultaneous conductances (black) or their shuffled counterparts (green). **e**, Signal-to-noise ratio of spike trains generated from simultaneous vs. shuffled conductances (dots). SNR for simultaneous conductances was 1.22 ± 0.04 times higher than that for shuffled conductances ($p = 0.0015$, 7 cells).

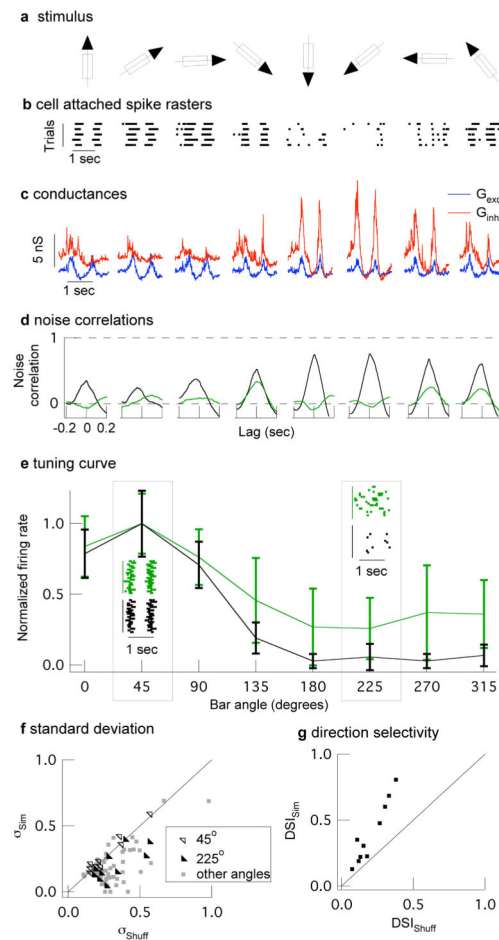


Figure 4. Strength and impact of noise correlations in synaptic inputs to On-Off direction-selective ganglion cells. **a**, A bar of light was moved in 8 directions, at 45° increments in random order. **b**, Cell-attached spike responses to the moving bar. **c**, Examples of simultaneously recorded conductances showing tuning of excitatory (blue) and inhibitory (red) conductances. **d**, Simultaneous conductances (black) show strong noise correlations that are largely absent in the non-simultaneous (green) conductances. **e**, Normalized directional tuning (spike count vs direction) from a single dynamic clamp experiment (mean \pm std) for 20 trials of simultaneous or shuffled simultaneous conductances. Insets at 45° (preferred direction) and 225° (non-preferred direction) show spike rasters. **f**, The standard deviation of the normalized spike count is significantly smaller for simultaneous compared to shuffled trials in non-preferred directions ($135\text{--}315^\circ$; $p < 0.05$, 10 cells). Standard deviations in the preferred direction were similar. **g**, The direction selective index (DSI; see Methods) is 2.0 ± 0.2 times larger for simultaneous compared to shuffled conductances ($p = 0.0002$, 10 cells).